Mathematical Model Formulation And Validation Of Water And Cryoprotective Agent Transport In Whole Hamster Pancreatic Islets

James D. Benson
Applied and Computational Mathematics Division
National Institute of Standards and Technology
Gaithersburg, MD, 20879

Charles T. Benson[*]
John K. Critser[†]
Comparitive Medicine Center
College of Veterinary Medicine
University of Missouri
Columbia, MO, 65211

Background: *Optimization of cryopreservation protocols for cells and tissues requres accurate models of heat and mass transport. Model selection often depends on the configuration of the tissue.*
Method of approach: *A mathematical and conceptual model of water and solute transport for whole hamster pancreatic islets has been developed and experimentally validated incorporating fundamental biophysical data from previous studies on individual hamster islet cells while retaining whole-islet structural information. It describes coupled transport of water and solutes through the islet by three methods: intracellularly, intercellularly, and in combination. In particular we use domain decomposition techniques to couple a transmembrane flux model with an interstitial mass transfer model.*
Results: *The only significant undetermined variable is the cellular surface area which is in contact with the intercellularly transported solutes,* A_{is}. *The model was validated and* A_{is} *determined using a* 3×3 *factorial experimental design blocked for experimental day. Whole islet physical experiments were compared with model predictions at three temperatures, three perfusing solutions, and three islet size groups. A mean of 4.4 islets were compared at each of the 27 experimental conditions and found to correlate with a coefficient of determination of* 0.87 ± 0.06 *(mean* $\pm$ *S.D.). Only the treatment variable of perfusing solution was found to be significant (*$p < 0.05$*).*
Conclusions: *We have devised a model that retains a significant amount of intrinsic geometric information about the system, and thus fewer laboratory experiments are needed to determine model parameters and thus to develop new optimized cryopreservation protocols. Additionally, extensions to ovarian follicles and other concentric tissue structures may be made.*
Keywords *perfusion; diffusion; cryobiology; multicellular mathematical modeling; mass transport; domain decomposition*

Nomenclature

L_{p}	Hydraulic Conductivity (μm min^{-1} atm^{-1})
P_{s}	Solute Permeability (μm min^{-1})
E_{a}	Activation energy (kCal/mol)
ω	Solute mobility ($P_{\mathrm{s}} = \omega RT$)
σ	Reflection coefficient
V	Cell volume (μm^3)
A	Surface area of cell (μm^2)
R	Gas constant (L atm K^{-1} mol^{-1})
T	Temperature (K)
S	Moles of permeating solute
C	Intracellular Concentration cryprotective agent (mol/kg)
K	Intracellular Concentration salt (mol/kg)
c	Extracellular Concentration cryprotective agent (mol/kg)
k	Extracellular Concentration salt (mol/kg)
$\overline{C}$	Mean concentration CPA (mol/kg)
J_s	Solute mole flux (mol/μm$^2/s$)
J_v	Volume flux (μm$/s$)
D	Solute diffusivity (μm/s^2)
λ	Tortuosity
t	Time (s)
R	Radius of whole islet (μm)
r	Radius from center of whole islet (μm)

[*]Current address: Eli Lilly & Co., Indianapolis, IN, USA.
[†]Address all correspondence to this author, email: critserj@missouri.edu

Introduction

The[1] effects of cryopreservation on cells and tissues can be better understood when account is made of the heat and mass transfer that occurs during each stage of the process. This understanding of what occurs on a cellular level may lead to increased survival through optimization of each cryopreservation step [2–4]. Although these processes have been well characterized for single cell suspensions [5, 6], published work on modeling these processes in multicellular tissues is relatively scarce.

For tissues, model selection is still an issue. For example, models have been constructed that describe water transport through a linear array of cells while neglecting transport through extracellular pathways [7]. Fidelman et al. [8] designed a model of isotonic solute-coupled volume flow in leaky epithelia using network thermodynamics to show how the Kedem and Ketchalsky mass transport parameters must behave in this system. Diller et al [9] utilized bond graphs and network thermodynamics to show that, depending on the transport resistance of the interstitium, the interior cell volume lags significantly behind the exterior cells. Subsequently Schreuders et al. [10] again used pseudo bond graph and network thermodynamics to model diffusion through a tissue and show that the effects of coupling on the multiple species present in the model is significant. Later, de Frietas et al. expanded a network thermodynamics model of transport in islet cells to model solute and solvent transport in islets of Langerhans [11].

Alternatively, cell-to-cell interactions are ignored and a model based on a diffusion equation with a phenomenological, experimentally determined, solute diffusivity [12–16]. These diffusion models may be appropriate for larger and denser tissues with a considerable number of cell layers. In fact, many alternate diffusion-based models have been proposed. For example, Xu et al [17] use a one dimensional porous media model to simulate solute transport in tissues, and Abazari et al. [18] construct a thermodynamically accurate tri-phasic model for articular cartilage. Another set of models are Krogh cylinder models [19] used primarily in organ perfusion systems [20, 21]. The Krogh cylinder model describes a cylindrical unit of tissue of fixed dimensions perfused by a capillary with a radius which varies with capillary volume. The solution behavior in diffusion models is well understood and usually simple to implement. Unfortunately, phenomenological diffusion constants depend on both the solute and the tissue structure, and thus applications are often restricted to experimental conditions in which measurements have been made.

Because islets are tissues with less than ten layers, it is computationally feasible to retain geometrical information. Using this idea, the present work builds upon these existing models, with the primary goal to model the mass transfer of solutes and solvents inside islets of Langerhans while retaining as much geometric information as possible. Note that the geometry of this model has clinically important analogues in other smaller tissues, such as ovarian follicles, a subject of current cryobiological research [22–24].

We first recreate the work of Levin [7] by modeling transport across an array of cells. However, we model the geometry of the layers as a series of concentric spheres, with each layer the thickness of the diameter of an individual islet cell, and we include the effects of a permeating solute using Kedem and Katchalsky's equations [25]. Next we construct a model to calculate the diffusion of a solute through a sphere of water, using the radially symmetric diffusion model with a tortuosity factor to reflect the interstitial matrix in a spherical tissue. Finally, we combine these models, accounting for both diffusion through the interstitium of the spherical array of layers and cell-cell osmosis. This allows solute and water transport into and out of the deeper layers of the sphere by one of two methods: serially through each of the overlying layers and across that portion of the cell membrane that is exposed to the intercellular transport driven by diffusion.

Previously published data for hamster islets of Langerhans [26, 27] supply many of the biophysical parameters. Here we show that the only previously undetermined variable that significantly affects the model is the cellular surface area that is in contact with the intercellularly transported CPA (A_{is}). The model is validated and A_{is} determined using a 3×3 factorial experimental design blocked for experimental day. Whole islet experiments are compared with model predictions at three temperatures (8, 22, 37 °C), using three perfusing solutions (DMSO, EG, 3×PBS), and three islet size groups ($< 80\mu$m, $80 - 110\mu$m, $> 110\,\mu$m radii). Using coefficient of determination (R^2) as our statistical measure, we show that our model provides an accurate description of volume excursion for whole islets in response to osmotic challenges.

1 Mathematical Model

1.1 Assumptions

The intra- and extracellular media are assumed to be ideal, hydrated, dilute multicomponent solutions and the membranes of the cells are simple and homogeneous. The equations which we use to analyze non-equilibrium fluxes of water and solute are based on the work of Kedem and Katchalsky (K/K) [25] which describe equations based on the assumptions of ideal and dilute solutions.

We will neglect concentration polarization, the effect of unstirred layers and advection due to transmembrane flux, on the permeability of the cells as Benson showed that for tissue of the size of islets of Langerhans there were significant effects of solute polarization only in the case where viscosities were high or in the presence of high fluid velocity fields [28]. We assume that adjacent membranes can be modeled as two independent membranes in series, resulting in a halving of effective hydraulic conductivity and solute permeability. An identical assumption was made in Levin et. al. [7] where they drew upon the work of Levin et al. [29] to demonstrate that little solute polarization occurs within the small volume of aqueous solution separating closely packed cells.

We assume that both the cell surface area in contact with other cells (A_c) and in contact with intercellular media (A_{is})

[1] Some of this work appeared as part of a doctoral dissertation [1]

are constant. The accuracy of this assumption is debatable (e.g. [30, 31]), however in general many investigators maintain constant surface area to avoid the problem of an increase in membrane surface area when the tissue expands past its isotonic volume [20, 21]. And we ignore intracellular diffusion effects, assuming that solute that enters a cell (layer) is distributed evenly across the cell (layer) volume. This assumption may be justified by the diffusion length given by $L_D = 2\sqrt{Dt_c}$, where D is the diffusivity, and t_c is a characteristic time. In particular, we have $D \approx 900\ \mu\text{m}^2/\text{s}$ (the approximate diffusivity of DMSO or ethylene glycol), and $t_c = 10$ s (the approximate time for equilibration of an individual islet cell). Thus $L_D = 2\sqrt{900 * 10} \approx 95\mu$m, which is significantly longer than the approximate islet cell radius of 6 μm, though not sufficiently long to discard for an entire islet of diameter approximately 100 μm. We show below that the complete model is relatively insensitive to the diffusivity, supported by this length.

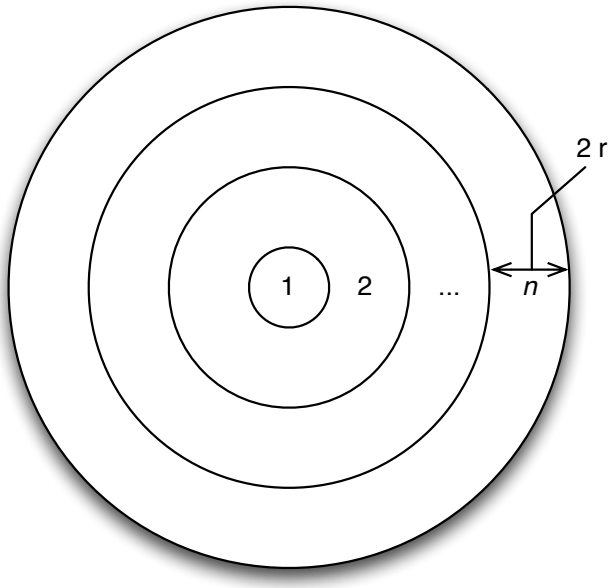

Fig. 1. The cell-to-cell transport model is constructed of concentric spheres of thickness equal to the diameter of an individual islet cell. The the cell-to-cell transport is assumed to be radially symmetric, and boundaries 1 through $n-1$ are modeled as two membranes in series, corresponding to halved permeability coefficients. The exterior boundary is exposed to the extra-islet concentration c^{e}.

1.2 Cell membrane mass transport model

Because parameter data for individual islets have already been published, we use the same formalism described by Kedem and Katchalsky, which gives the total volumetric mass flow J_v as well as the permeable non-electrolyte (e.g. DMSO) mass flow J_s across a membrane in terms of the phenomenological coefficients L_{p}, ω, and σ [25]:

$$\begin{aligned} \frac{dV}{dt} &= J_v(c,C,k,K)A = -L_pART\left(k-K+\sigma(c-C)\right), \\ \frac{dS}{dt} &= J_sA = (1-\sigma)\overline{C}J_v + \omega(c-C), \end{aligned} \tag{1}$$

where all parameters are defined in the Nomenclature section, and $\overline{C_{\text{CPA}}}$ is the average of extracellular and intracellular CPA concentrations (osmolality) defined by Kedem and Ketchalsky,

$$\overline{C_{\text{CPA}}} = (c-C)/[\ln(c/C] \approx (c+C)/2.$$

The intracellular concentrations of salt and CPA during anisosmotic conditions were determined from the Boyle Van't-Hoff relation applied to the osmotic responses of cells [27, 32].

Finally, it will be convenient later to note that $C := S/V$, and system (1) may be rewritten as follows, with J_w and J_s defined as above

$$\begin{aligned} \frac{dV}{dt} &= J_vA, \\ \frac{dC}{dt} = \frac{d(S/V)}{dt} &= \frac{J_sAV - J_vAS}{V^2}. \end{aligned} \tag{2}$$

1.3 Intracellular transport model

The mass transport model (1) was applied to the geometry shown in Fig. 1. This model is a series of concentric spheres and is built by assuming that the innermost sphere (sphere 1) is of the dimensions and volume of a single hamster islet cell (approximately 12.2 μm in diameter and 960 μm^3 in volume). Each surrounding layer is the thickness of the diameter of one islet cell. All layers have water and solute permeabilities equal to $0.5L_{\text{p}}$ and $0.5P_{\text{s}}$ except for the outermost layer, with permeabilities simply equal to L_{p} and P_{s}. We then set L_{p} and E_{a} of L_{p}, P_{s} and E_{a} of P_{s}, and σ equal to values found for hamster islet membranes for DMSO and EG [26]. The nonosmotically active portion V_{b} of the cells (layers) was also set to be 0.40 from previous experiments [27]. p

1.3.1 Results

Figure 2 shows the results of modeling of a seven layer intracellular transport model (approximately 150 μm in total diameter) where the extra-islet concentration was fixed at 1.5 mol/kg DMSO. The first two plots (A and B) show the water volume and DMSO concentration in each of the seven layers, respectively and the third plot (C) shows the total islet model water volume (μm^3) as a function of time. Transport is delayed in interior layers and subsequently whole islet equilibration takes over 1000 seconds.

1.4 Intercellular transport model

We next construct a model of inter-islet transport modeled solely by diffusion, where the entire membrane of each cell in the islet is available to a local concentration modeled by free diffusion. Using the assumption of independent flow,

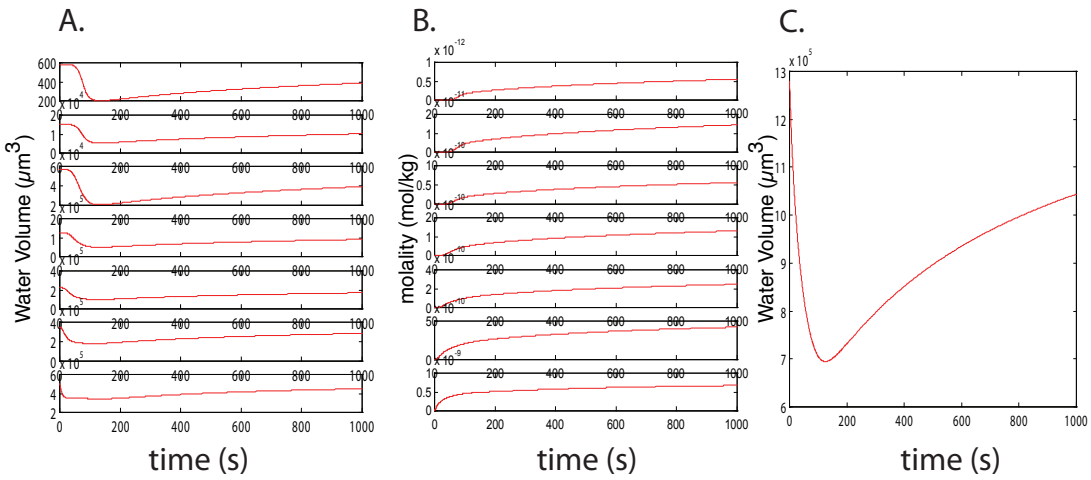

Fig. 2. The results of a seven layer model of approximately 150 μm in total diameter without interstitial diffusion, subjected to perfusion with 1.5 mol/kg DMSO. In this model solute and water transport take place exclusively across layer membranes. Plots A and B show the water volume (μm^3) and molality (mol/kg) as a function of time (seconds) of each of the seven layers with the interior at the top. Plot C shows overall model islet water volume (μm^3) (x-axis) as a function of time.

isothermal conditions, and with concentration independent diffusivity, we may use the standard linear diffusion equation in a sphere [33], coupled with initial and boundary conditions:

$$\begin{aligned} \frac{\partial c}{\partial t} &= \bar{D}\left(\frac{\partial^2 c}{\partial r^2} + \frac{2}{r}\frac{\partial c}{\partial r}\right), \\ c(r,0) &= c_0(r), \\ c(R,t) &= c^e(t). \end{aligned} \tag{3}$$

Here c is the concentration of solute in moles/kg, D is the diffusion coefficient in μm^2/sec, r is radius in μm, and t is time.

The diffusion coefficient D for a freely diffusing solute in water and that for a solute in the tissue interstitium should be different. However the choice of an appropriate model is unclear. For example, a porous media model may be appropriate [17], or more complicated relationships between chemical potential and strain may be developed [18]. We ignore these complications and use the linear diffusion model (3) with a constant diffusion coefficent for two reasons. First, for simplicity, the overall model will be of sufficient complexity that we hoped to only provide a level of detail as to what truly effects the overall outcome of the model. Second, we are able to demonstrate that the model itself is relatively insensitive to the overall diffusion coefficient.

We account for the specific geometry of islets by employing a tortuosity factor λ that scales the diffusivity constant. Specifically, the tortuosity factor is the actual length of the diffusion path per unit of length of diffusion moreover this factor is a function of tissue geometry and therefore is solute independent. Maroudas et al. [34] have shown that for diffusion through articular cartilage, D ranges from 603 μm^2/sec for urea (MW = 60.03 daltons) to 63 μm^2/sec for sucrose (MW = 342.3 daltons) at 22 °C. Further, it was found that articular cartilage has a tortuosity factor of 1.35. Page et al. [35] conducted experiments on cat heart muscle which, arguably, has a histology more similar to islets than cartilage. They found a range of diffusion coefficients of $D = 830\,\mu$m^2/sec for glycerol (MW=92.02 daltons) to $D = 262\,\mu$m^2/sec for sucrose (MW=342 .3 daltons) at 22 °C. It was shown that the temperature dependence was Arrhenius with an activation energy E_a of 5.46 Kcal/mole. Maroudas found tortuosity λ to be between 1.38 and 1.44.

Based on the above information we modified the above diffusion model to account for diffusion through an islet. Based on the molecular weight of DMSO (78.13 daltons) and EG (62.07 daltons) we assume the respective diffusion coefficients to be approximately 800 μm^2/sec with an activation energy $E_a = 5.46$ Kcal/mole. Further, we choose to use the extremal tortuosity of 1.44.

When examining the final model which includes solute uptake from the diffusion channels in the intercellular space it can be seen that the overall model is not very sensitive to D or λ. This is demonstrated by comparing whole islet equilibration using extreme values for D and λ. In particular, we set $D = 200\,\mu$m^2/sec and $\lambda = 1.44$, and $D = 982\,\mu$m^2/sec and $\lambda = 1$ in two numerical experiments, respectively. In the former experimental model whole islet intercellular equilibration occurred in about 20 seconds versus approximately 12 seconds in the latter model (c.f. Fig. 3). Further, the whole islet volume versus time curves for these conditions and assumptions were visually identical (data not shown). Therefore, a relatively large difference in D or λ yields an almost indistinguishable difference in the model.

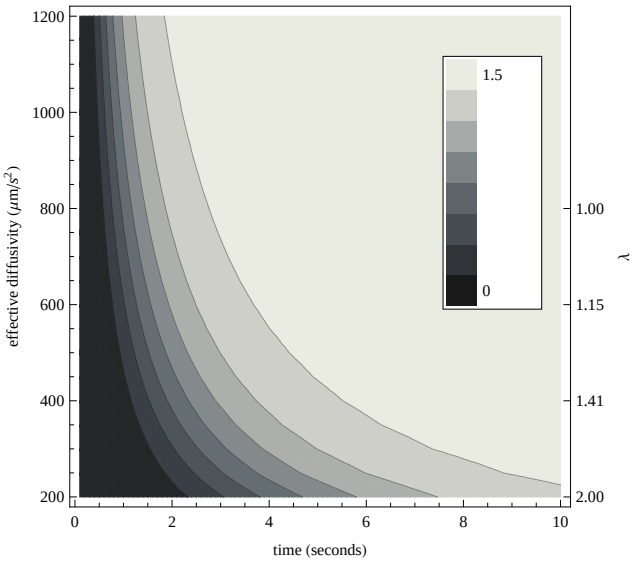

Fig. 3. Concentration at the center of a sphere of radius 80 μm as a function of time and effective diffusivity $\bar{D} = D/\lambda^2$. On the rightmost axis, totuosity is shown for the nominal $D = 800\,\mu$m/s^2.

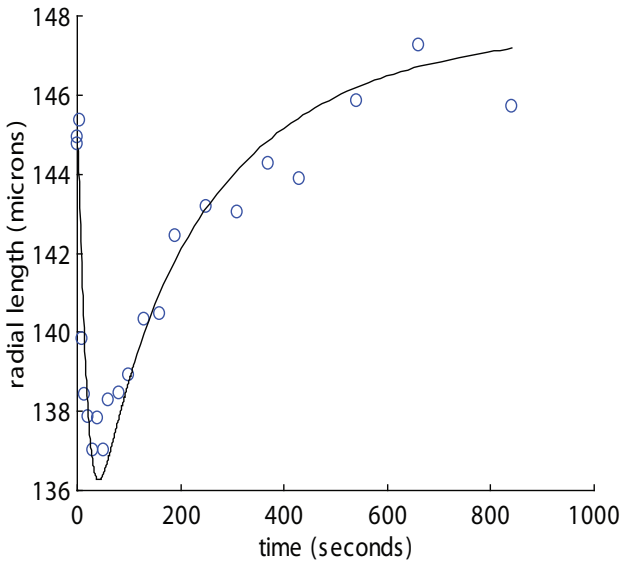

Fig. 4. Representative plot of radius vs. time for a whole hamster islet perfused with 1.5mol/kg DMSO at 22 °C. The solid line is model predictions under the same experimental conditions. The best fit channel radius (corresponding to A_{is}) for was 2.92 μm and correlation coefficient (R^2) was .91.

1.5 Combination model

The results of the model outlined in section 1.3 demonstrate that given the membrane characteristics for individual hamster islet cells, an entire islet with no intercellular transport perfused with 1.5 mol/kg DMSO would take greater than 1000 seconds to equilibrate. On the other hand, if the islet could truly be modeled as a "bunch of grapes," with each cell completely exposed to interstitial diffusion, the behavior would be dependent on the diffusion characteristics of a sphere outlined in section 1.4. Since the results from that section showed that the sphere would be equilibrated in a relatively small time (regardless of the diffusion coefficient and tortuosity factor), whole islets should equilibrate on the same time scale as individual islet cell. Further, if an islet was truly a "bunch of grapes" its behavior would be reasonably independent of the size of the islet, for the same reasons outlined above.

Benson et al. [26] showed that an individual cell perfused with 1.5 mol/kg DMSO at 22 °C would equilibrate in less than 150 seconds. Therefore under a pure diffusion model, the whole islet would follow a similar time course as an individual islet cell. In fact, physical experiments below show that when an islet of approximately 150 μm diameter is exposed to 1.5mol/kg DMSO the equilibration takes about 600 seconds (see Fig 4). Furthermore, the size of the islet does affect the equilibration time. Therefore, the behavior of the hamster islet must be a combination of the two extremes. It must have some intercellular (interstitial) transport, but not all cells are completely exposed to this intercellular solute. We have therefore chosen to develop the "combination" model which follows.

1.5.1 Modeling

The concept for the combination model can be seen in Fig. 5. The geometry of this model is again concentric cell layers with volumes and membrane areas calculated from the cell-to-cell concentric spherical model, but with cylindrical channels evenly distributed throughout the tissue. Solute diffusion through these channels is calculated using the diffusion equations from the previous diffusion model, though we make the notable exception that locally the concentration of solute in the interstitium is affected by the flux across the interstitial cell membrane (defined by boundaries B^i) with which it is adjacent, according to the K/K equations.

In this model we assume that the extracellular (interstitial) volume of the islet remains fixed at 20% of the overall islet volume throughout the experimental perfusion. The value of approximately 20% has been published by several studies on tissues [35–37]. However, the actual value is not as important as the concept of the ratio of intra- and extracellular space being fixed. This assumption is supported by the experiments conducted in Benson et al. [26] and Liu et al. [27] which demonstrated that the V_{b} of individual cells is approximately 40% and the apparent V_{b} of the whole islet is also approximately 40%. These data lead to the conclusion that since the respective Boyle Van't Hoff plots (normalized volume vs. 1/Osmolality) for individual islets and whole islets are identical, the extracellular volume of the islet must remain in direct proportion to the overall islet volume, supporting the above assumption.

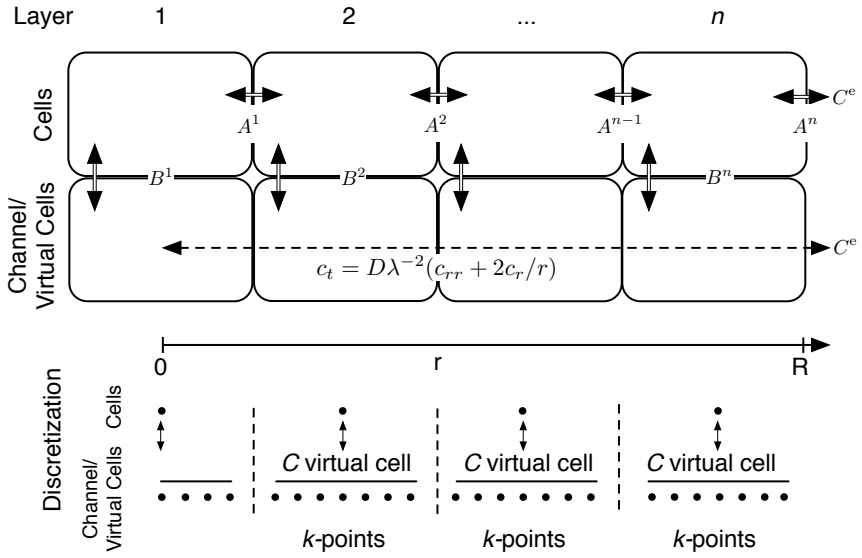

Fig. 5. Conceptual model of the combination of diffusion and cell-to-cell transport. Double lines indicate mass transport governed by the Kedem and Katchalsky (K/K) model, whereas the dashed line indicates mass transport governed by the diffusion equation in a sphere with tortuosity factor λ. At membrane interfaces A_i, $i = 1,\ldots,n-1$, we model transport as two membranes in series, resulting in a halved effective cell-to-cell permeability. At membrane interfaces B_i, $i = 1,\ldots,n$, the exterior local concentration governing mass transport at the ith cell depth is given by the mean concentration in the "virtual cell." Spatial discretization is also shown.

1.5.2 Interstitial surface area ($A_{\rm is}$)

There is no clear choice of how to conceptually represent the interstitium. This conceptual model is necessary in order to mathematically calculate the volumes and surface areas of our various components. Here we model the extracellular space within the islet as a series of cylinderical channels penetrating the spherical model and occupying a constant 20% of the overall islet volume. The sum of cell volumes is set at 80% of the volume defined by the concentric sphere model. The surface area of each concentric layer (boundaries $A^1,\ldots,A^n$ in Fig. 5) is calculated from the cell-to-cell transport model with the cross-sectional area of the channels removed. First, to calculate the number of channels, we have the volume of one channel, $V_{channel} = \pi\delta^2 R$,which, in turn allows us to calculate the number p of channels comprising 20% of the total islet volume $p = 0.2V_{islet}/V_{channel}$,and thus the constant total channel area $A_{\rm is} = p(2\pi\delta)$. It is convenient to define the normalized $A_{\rm is}$ by dividing by the total cellular surface area

$$\overline{A_{\rm is}} := A_{\rm is}\frac{V_{cell}}{0.8V_{islet}A_{cell}}.$$

This ratio is fixed for all cells and all time.

Finally, we note that the total cellular surface area is based on the calculated surface area of an individual spherical islet cell in suspension. Because this cell has a minimal surface area to volume ratio, we expect that because cells in tissues are aspherical and their physiologic volume is the same, the effective surface area of cells in a tissue construct should be higher. This implies that, though based in a theoretical framework, the above quantity is phenomenological and values should not indicate the "true" ratio of interstitial surface area to intercellular surface area.

1.5.3 "Virtual" Cells

The final question is how to treat the interaction between cells and their adjacent channels. The transmembrane volume flux at B^i is governed by a mean concentration along this membrane, but we wished to include the effects of solute and solvent mass transfer on the local concentration in the channels. One possibility would be to create a piecewise defined Robin boundary condition to account for the flux along boundary $B = \cup_{i=1}^n B^i$, and solve the diffusion equation in a two dimensional channel. At this length scale, however, the diffusion normal to the cell membrane and across the channel should be nearly instantaneous and the local concentration would be influenced only by the radial diffusion and the normal boundary conditions defined by the K/K model.

In practice, this should be identical to the application of so called "virtual" cells (see Fig. 5). We assume that the transmembrane flux across any boundary B^i is governed by the mean local concentration governed by diffusion. This flux then affects the local concentration independent of diffusion. Numerically, this is achieved by performing a domain decomposition in r [38] in the channel with each layer constituting a new domain and coupling these layered domains to their associated cell layers using the K/K model by assuming that the concentration of a virtual cell associated with this domain is equal to the average of the concentrations of the nodes adjacent to an islet layer (see discretization in Fig. 5), and the volume of a virtual cell equal to 20% of the associated cell-layer volumes.

We now can define the complete model. Suppose that we have the configuration in figure 5. Let $\Omega = [0,R]$, and partition Ω into disjoint subdomains Ω_i such that $\Omega = \cup_{i=1}^{n} \Omega_i$. Let $c_i : \Omega_i \times [0,\infty) \to [0,\infty)$ be the concentration in the channel in the ith domain and $W_i, C_i : [0,\infty) \to [0,\infty)$ be the water volume and concentration in the ith cell layer, be defined by the system of coupled reaction-diffusion and ordinary differential equations (note that we use capital and lowercase variables for intra and extracellular quantities, respectively):

$$\begin{aligned}
\frac{\partial c_i}{\partial t} &= D_i\left(\frac{\partial^2 c_i}{\partial r^2} + 2\frac{\partial c_i}{\partial r}\right) + f_c^i(\bar{c}_i, C_i, W_i) \text{ in } \Omega_i \times (0,\infty),\\
\frac{dW_i}{dt} &= f_w^i(\bar{c}_i, C_i, C_{i-1}, C_{i+1}, W_i),\\
\frac{dC_i}{dt} &= f_C^i(\bar{c}_i, C_i, , C_{i-1}, C_{i+1}, W_i),
\end{aligned}$$

supplemented with initial and boundary conditions (with $\Gamma_i := \partial\Omega_{i-1} \cap \partial\Omega_i$):

$$\begin{aligned}
c_i &= c_0 \quad \text{in } \Omega_i \times \{0\},\\
c_i &= c_{i-1} \quad \text{in } \Gamma_i \times [0,\infty), i > 1,\\
\frac{\partial c_i}{\partial r} &= \frac{\partial c_{i-1}}{\partial r} \quad \text{in } \Gamma_i \times [0,\infty), i > 1,\\
\frac{\partial c_i}{\partial r} &= 0 \quad \text{in } \partial\Omega \times [0,\infty),\\
c_n &= c^e(t) \quad \text{in } \partial\Omega \times [0,\infty),\\
W_i(0) &= W_i^0,\\
C_i(0) &= C_i^0,
\end{aligned}$$

where $\bar{c}_i := \frac{1}{|\Omega_i|}\int_{\Omega_i} c_i\,dx$ is the mean extracellular concentration at the ith level, and $c^e : [0,\infty) \to [0,\infty)$ is the extra-islet concentration. Note that we assume that there is only a single diffusing species. In other words, if the extratissue salt concentration is fixed at isotonic, then the salt concentration will be uniform throughout the numerical experiment. If the extratissue salt concentration is non-isotonic, then we do not model the diffusion of permeating solute species.

Finally, we define the reaction terms $f^i : \mathbb{R}^k \to \mathbb{R}$ which stem from the K/K formalism. From system (2), we may define the reaction terms and ODEs

$$f_c^i = J_s(c_i, C_i)\frac{A_{is}}{0.2V_i} + J_w(c_i, C_i, k_i, K_i)\frac{c_i A_{is}}{0.2V_i}, \tag{4}$$

$$\begin{aligned}
f_w^i &= J_w(C_i, c_i)A_{is} + J_w(C_i, C_{i-1}, K_i, K_{i-1})\frac{A}{2}\\
&\quad + J_w(C_i, C_{i+1}, K_i, K_{i-1})\frac{A}{2},
\end{aligned} \tag{5}$$

$$\begin{aligned}
f_C^i &= J_s(C_i, c_i)\frac{A_{is}}{V_i} + J_w(C_i, c_i, K_i, k_i)\frac{c_i A_{is}}{V_i}\\
&\quad + J_s(C_i, C_{i-1})\frac{A}{V_i} + J_w(C_i, C_{i-1}, K_i, K_{i-1})\frac{C_i A}{2V_i}\\
&\quad + J_s(C_i, C_{i+1})\frac{A}{V_i} + J_w(C_i, C_{i+1}, K_i, K_{i+1})\frac{C_i A}{2V_i},
\end{aligned} \tag{6}$$

where $J_w(c,C,k,K)$ and $J_s(c,C)$ are defined in display (1).

1.5.4 Summary

We have built a combination model which provides for effects of intra- and inter-stitial transport within our conceptual islet. In fact, the only unknown variable in this model is $\overline{A_{\text{is}}}$. Therefore, when we validate and test the model in the study which follows, we will let $\overline{A_{\text{is}}}$ be our only floating variable.

2 Materials and Methods

2.1 Reagents

Unless stated otherwise, all chemical reagents were obtained from Sigma (St. Louis, MO). Collagenase P was purchased from Boehringer Mannheim (Indianapolis, IN). Cell culture reagents, including Hanks' balanced salt solution, Medium 199, fetal bovine serum (FBS) and 0.25% trypsin-EDTA, were purchased from Gibco (Gaithersburg, MD)[2]

2.2 Isolation of Islets From Hamsters

Hamster pancreatic islets were isolated as previously described by Gotoh et al. [39]. Briefly, 6-8 wk old golden hamsters (Harlan Sprague Dawley, Indianapolis, IN) were anesthetized via inhalation of Forane (Isoflourane; Ohmeda Caribe inc.; Guayama PR). The common bile duct was cannulated under a stereomicroscope with a polyethylene catheter through which approximately 8-10 ml of cold (1-4 °C) M-199 medium containing 0.5 mg/ml of collagenase P was injected slowly until whole pancreas was swollen. The pancreas was excised and digested at 37 °C for approximately 50 min in M-199 medium containing 100 mg/ml of penicillin G and 100 mg/ml of streptomycin (no additional collagenase). The digest was washed three times in cold M-199 medium and passed through a sterile 500 mm stainless steel mesh. Islets were purified by centrifugation through a Ficoll density gradient (1.037, 1.096 and 1.108) at 800 g for 20 min.

2.3 Perfusion of Islets and measurement of resulting volume excursions

The design and structure of the microperfusion chamber system is similar to that described elsewhere [40]. Briefly, the experiments were conducted by introducing 2 -10 islets into the chamber cavity (height: 1 mm, diameter:2 mm, volume: 3.14 μl) using the Hamilton syringe. With application of negative pressure from below, the solution moved out of the chamber, but the islets remained on the transparent porous membrane at the bottom of the cavity (polycarbonate screen membrane; Poretics Co., Livermore, CA; membrane thickness: 10 μm, pore diameter: 5 μm, pore density: 4×10^5

[2]Certain commercial equipment, instruments, or materials are identified in this paper in order to specify the experimental procedure adequately. Such identification is not intended to imply recommendation or endorsement by the National Institute of Standards and Technology, nor is it intended to imply that the materials or equipment identified are necessarily the best available for the purpose.

pores/cm^2). Next, 700 μl of a perfusion medium was loaded in the reservoir at the solution inlet and approximately 400 μl was perfused through the chamber by aspiration via a 1 ml syringe. The reservoir (with 300 μl of remaining solution) was then sealed via application of a glass cover slip, ensuring no evaporative effects. The entire perfusion took place in less than eight seconds and the original isotonic solution in the perfusion chamber cavity (3.14 μl) was quickly replaced over 100 times by the new perfusion medium, ensuring that none of the original isotonic solution remained in the chamber and that back diffusion of original solution into the chamber was impossible. Cells were immobilized by the downward flow of the perfusion medium during the perfusion process facilitating the recording of cell volume changes by a video camera.

The perfusion chamber and cell suspension cavity were cooled/heated with a temperature controller to reach an equilibrium. The prepared perfusion media was precooled or heated in a temperature-controlled methanol bath (Digital Temperature Controller, Model 9601, Polyscience Co., Niles, IL) to the same temperature as the perfusion chamber. Precooled/heated media was then perfused into the chamber and around the cell(s). During the experiment, the temperature variation of the perfusion medium and of the microperfusion chamber were monitored and the range of temperature difference between the perfusion medium and the chamber was $\pm 0.2\ ^\circ$C during experiments (data not shown).

Individual video frames were imported into SigmaScan/Image version 1.20.09 (Jandel Corporation, San Rafael, CA). Islets were then outlined and area was measured by filling this outline. All islets used in this study were roughly spherical (unpublished data). A radius was then computed using this assumption of a spherical shape. Images were calibrated by measurement of spherical polyethylene beads (92.12 μm diameter, Coulter corporation, Epic division, Hialeah, FL).

The coupled system of partial and ordinary differential equations were discretized spatially as shown in Fig 5, and the resulting ordinary differential equations were simultaneously solved using MATLAB (The MathWorks, Natick, MA) function "ode45." Best fit for A_{is} was found using MATLAB function "fmins" which uses a modified simplex search method.

Model predictions were compared to experimental data using coefficient of determination (R^2) calculations, and ANOVA wes performed using the General Linear Models (GLM) computational procedure of the Statistical Analysis System (SAS; SAS Institute, Inc., Cary, NC). This procedure partitioned the variance of the three main treatment effects: temperature, islet size, and perfusing solution as well as the two way interaction effects. Further, the 3×3 factorial experiment was also blocked by day. Therefore, day was included in the SAS GLM model which allowed it to remove variability due to day to day variation. Significance of main effect was tested using the appropriate mean squares (Temperature effect tested by Temperature $\times$ Day interaction as the error term, etc.).

3 Results and Discussion

A model was developed to describe the behavior of islets of Langerhans in the golden hamster when they are exposed to anisosmotic conditions. The model was validated and A_{is} determined using a 3×3 factorial experimental design which was blocked for experimental day. Whole islet in vitro experiments were compared with model predictions at three temperatures, using three perfusing solutions and three islet sizes.

3.1 Correlation of model with experimental data

Typical results for correlation of several of the experimental protocols are shown in Figs. 4 and 6. These figures include data from in vitro perfusion experiments using the three perfusion media (1.5 mol/kg DMSO, 1.5 mol/kg EG, and $3\times$ PBS) and hamster islets of Langerhans. Superimposed on this data is the prediction of the mathematical model described above. Table 1 contains the combined data from all of the 27 experiments performed for this study.

A mean of 4.4 islets were compared at each of the 27 experimental conditions and found to correlate with a coefficient of determination (R^2) of 0.87 ± 0.06 (mean $\pm$ S.D.). This excellent value for R^2 demonstrates that, even with only one fitting variable, the model predicts the experimental data with a high degree of accuracy. The remaining 13% of the variability could possibly be explained by error in measurement.

3.2 Day Effect

The 3×3 factorial design was blocked for day and when using analysis of variance (ANOVA) for A_{is}, it was found that this day effect was significant ($p < .05$). This indicates that there is significant day to day variability of A_{is} for hamster islets. This variability may be explained by hamster to hamster variability, or by day to day isolation variability. Hamster to hamster variability was seen for hamster oocyte water permeability and activation energy [41]. However, it is more likely that even slight differences in digestion of the islets in collagenase from day to day could affect the A_{is} significantly. Visually, increased digestion renders some islets "looser" (Dr. Raymond Rajotte, personal communication) which could hypothetically increase A_{is}.

3.3 Interstitial surface area (A_{is})

The $\overline{A_{is}}$ from 119 islets (10 hamsters over 5 experimental days) was found to have a mean of 0.54 ± 0.34 (mean $\pm$ S.D.) across all treatments. Values greater than one may seem at first to be counter-intuitive. However, we normalized our value of A_{is} to spherical internal individual islet cells, which have a minimal surface area to volume ratio. Therefore, non-spherical cells inside the islet would increase the overall surface area to volume ratio and increase the total membrane surface area of the islet, thus decreasing our normalized A_{is}.

We also compared A_{is} over experimental conditions using ANOVA and found the treatment variable of perfusing

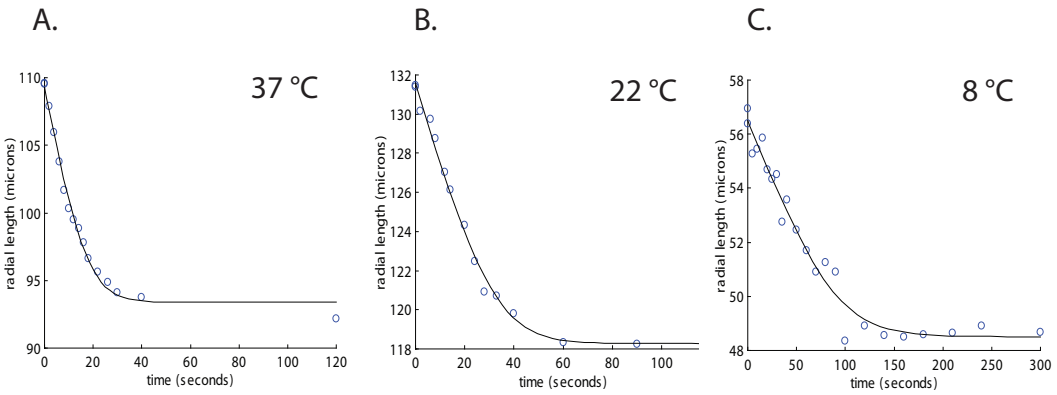

Fig. 6. Plots of islets with various radii perfused with $3\times$ PBS at 37, 22, and 8 $^{\circ}$C. The solid line is model predictions under the same experimental conditions. The best fits for channel radius (corresponding to $A_{\rm is}$) were 1.79, 2.08, 1.21 μm and correlation coefficients (R^2) were 0.99, 0.99, 0.97, respectively.

Table 1. Data from the $3\times$ 3 factorial experiment is shown where whole islets were compared with model predictions at three tempreatures (7, 22, 37 $^{\circ}$C) using three perfusing solutions (DMSO, EG, and 3 $\times$ PBS) and three islet size groups ($<$80, 80-110, $>$110, μm radii).

CPA	Temp. ($^{\circ}$C)	radius (μm)	# of islets	initial radius (μm) mean	S.D	Normalized $A_{\rm is}$ mean	S.D.	coeff. of det. mean	S.D.
DMSO	37	<80	3	69.98	7.56	0.34	0.07	0.77	0.10
DMSO	37	$80-110$	4	95.94	9.85	0.28	0.13	0.78	0.10
DMSO	37	>110	3	120.07	6.49	0.39	0.14	0.81	0.16
EG	37	<80	3	75.58	14.36	0.34	0.02	0.88	0.04
EG	37	$80-110$	4	91.74	3.28	0.20	0.04	0.90	0.02
EG	37	>110	3	121.53	23.72	0.24	0.11	0.62	0.27
PBS	37	<80	3	70.12	7.81	0.41	0.31	0.96	0.03
PBS	37	$80-110$	3	100.79	8.19	0.50	0.16	0.99	0.00
PBS	37	>110	2	122.80	9.48	0.48	0.09	0.96	0.03
DMSO	22	<80	2	76.64	6.82	0.22	0.13	0.76	0.15
DMSO	22	$80-110$	3	92.71	11.03	0.30	0.12	0.89	0.03
DMSO	22	>110	3	123.27	17.97	0.22	0.14	0.89	0.12
EG	22	<80	4	66.54	2.37	0.59	0.19	0.82	0.02
EG	22	$80-110$	3	86.58	10.62	0.42	0.08	0.85	0.00
EG	22	>110	2	111.85	0.78	0.42	0.22	0.72	0.04
PBS	22	<80	8	56.21	15.31	1.12	0.87	0.92	0.05
PBS	22	$80-110$	8	88.78	10.58	1.01	0.25	0.96	0.02
PBS	22	>110	5	120.80	10.29	0.43	0.25	0.97	0.02
DMSO	8	<80	6	53.48	14.44	0.48	0.10	0.86	0.07
DMSO	8	$80-110$	5	93.16	7.16	0.41	0.01	0.87	0.07
DMSO	8	>110	4	125.03	23.67	0.42	0.05	0.93	0.04
EG	8	<80	4	65.13	14.02	0.45	0.11	0.80	0.08
EG	8	$80-110$	5	91.21	8.66	0.42	0.03	0.88	0.05
EG	8	>110	4	117.38	12.40	0.39	0.01	0.79	0.07
PBS	8	<80	10	59.30	8.36	1.44	0.56	0.96	0.02
PBS	8	$80-110$	9	88.77	10.61	1.40	0.37	0.98	0.01
PBS	8	>110	6	121.77	16.10	0.93	0.29	0.99	0.01
		Mean	4.41	92.86	10.81	0.54	0.18	0.87	0.06
		St. Dev	2.15			0.34		0.09	

solution to be significant ($p < .05$). Furthermore, ANOVA with multiple comparisons demonstrated that A_{is} for PBS is greater than for DMSO or EG exposure ($p < .05$). This seems to suggest that the islets, when exposed to 3×PBS, have more surface area exposed to the interstitial diffusional transport than when they are exposed to DMSO or EG. A possible hypothesis is that there are areas of the islet which water is able to diffuse out of (in the case of hypertonic PBS perfusion) but larger molecules such as DMSO and EG are excluded from. This hypothesis is supported by the work of Barr et al. [42] who showed that the apparent extracellular spaces of smooth muscle decreased with increasing molecular size. Further, Bunch et al. [43] found that only 60% of total water to be available to DMSO in barnacle muscle. A second explanation may be that the two CPAs affect the histology of the islet in such a way as to "tighten" it and make it less susceptible to diffusional effects. Further exploration of this area may be warranted.

Alternatively, the lack of significant differences in A_{is} in the CPA groups EG and DMSO point to the conclusion that A_{is} is a truly geometrically dependent parameter. This conclusion would indicate that our model has captured more information than a strictly phenomenlogical diffusion based model. Because of this, predictions based on knowledge of this parameter and knowledge of the diffusivities for other CPAs may be made without experimental measurements.

4 Applications

This validated model may now be used to predict several stages in the cryopreservation process. For example, these predictions may include the degree of volume excursion of each layer in response to exposure to CPAs or other hyper and hypotonic solutions. It has been shown that rate of introduction and removal of CPAs is important to the successful preservation [44–46] both volume excursion (swelling or shrinking) and/or solute effects may be important in cell survival [47]. Combined with equations published for solute/solvent dynamics at low temperatures [9,20,21,48] both the concentration of CPA within each layer at the time of freezing, and the concentration of water within the cells at the time of ice nucleation may be predicted. These values have also been shown to be of great importance to the overall outcome of the cryopreservation procedure [5,6,49]. There also has been recent discussion on the ice propogation in concentrically oriented tissues, where solute and solvent transport have been neglected [50, 51]. It would be of considerable interest to apply the intracellular ice and propogation theory discussed in these papers in combination with the model described and validated in this manuscript.

5 Summary

A model has been constructed that accurately predicts volume excursion in response to osmotic and CPA challenges for whole islets while maintaining geometric information about the behavior of the entire islet. This model incorporates data describing fundamental biophysical characteristics from previous studies on individual hamster islet cells and describes transport through the islet by three methods: intracellularly, intercellularly, and a combination of these. Development of optimal cryopreservation protocols using this information remains to be accomplished.

Funding Funding for this research was provided by the University of Missouri, NIH grants U42 RR14821 and 1RL 1HD058293 (J.K. Critser PI), and the National Institute of Standards and Technology National Research Council postdoctoral associateship (J.D. Benson).

References

[1] Benson, C. T., 1996. "Fundamental cryobiology of pancreatic islets of langerhans". PhD thesis, Indiana University, July.

[2] Mazur, P., Cole, K. W., Hall, J. W., Schreuders, P. D., and Mahowald, A. P., 1992. "Cryobiological preservation of drosophila embryos". *Science,* **258**(5090), Dec, pp. 1932–1935.

[3] Whittingham, D., Mazur, P., and Leibo, S. P., 1972. "Survival of mouse embryos frozen to -196 degrees and -269 degrees C". *Science,* **178**(4059), pp. 411–414.

[4] Benson, C. K., Benson, J., and Critser, J., 2008. "An improved cryopreservation method for a mouse embryonic stem cell line". *Cryobiology,* **56**, pp. 120–130.

[5] Levin, R. L., Cravalho, E. G., and Huggins, C. E., 1976. "Membrane model describing effect of temperature on water conductivity of erythrocyte-membranes at subzero temperatures". *Cryobiology,* **13**(4), pp. 415–429.

[6] Mazur, P., 1990. "Equilibrium, quasi-equilibrium, and nonequilibrium freezing of mammalian embryos". *Cell Biophys,* **17**(1), Aug, pp. 53–92.

[7] Levin, R. L., Cravalho, E. G., and Huggins, C. E., 1977. "Water transport in a cluster of closely packed erythrocytes at subzero temperatures". *Cryobiology,* **14**(5), pp. 549–558.

[8] Fidelman, M. L., and Mikulecky, D. C., 1988. "Network thermodynamic analysis and simulation of isotonic solute-coupled volume flow in leaky epithelia - an example of the use of network theory to provide the qualitative aspects of a complex system and its verification by simulation". *Journal of Theoretical Biology,* **130**(1), Jan, pp. 73–93.

[9] Diller, K. R., and Raymond, J. F., 1990. "Water transport through a multicellular tissue during freezing - a network thermodynamic modeling analysis". *Cryo-Letters,* **11**(2), Mar-Apr, pp. 151–162.

[10] Schreuders, P. D., Diller, K. R., Beaman, J. J., and Paynter, H. M., 1994. "An analysis of coupled multicomponent diffusion in interstitial tissue". *Journal of Biomechanical Engineering,* **116**(2), May, pp. 164–71.

[11] de Frietas, R. C., Diller, K. R., Lachenbruch, C. A., and Merchant, F. A., 1998. "Network thermodynamic model of coupled transport in a multicellular tissue the islet of langerhans". In Biotransport: heat and mass transfer in living systems, K. R. Diller, ed., Vol. 858 of *Annals of the New York Academy of Sciences*, pp. 191–204.

[12] Isbell, S., Fyfe, C., Ammons, R., and Pearson, B., 1997. "Measurement of cryoprotective solvent penetration into intact organ tissues using high-field NMR microimaging". *Cryobiology,* **35**(2), pp. 165–172.

[13] Fuller, B., and Busza, A., 1994. "Proton NMR studies on the permeation of tissue fragments by dimethyl sulphoxide: liver as a model for compact tissues (Accepted February 7th, 1994)". *Cryo-Letters,* **15**(2), p. 131.

[14] Devireddy, R., Coad, J., and Bischof, J., 2001. "Microscopic and calorimetric assessment of freezing processes in uterine fibroid tumor tissue". *Cryobiology,* **42**(4), JUN, pp. 225–243.

[15] Han, X., Ma, L., Benson, J., Brown, A., and Critser, J. K., 2009. "Measurement of the apparent diffusivity of ethylene glycol in mouse ovaries through rapid MRI and theoretical investigation of cryoprotectant perfusion procedures". *Cryobiology,* **58**(3), Jun, pp. 298–302.

[16] Han, X., Liu, Y., Benson, J. D., and Critser, J. K., Submitted. "A calorimetric method to measure water-cryoprotectant mutual diffusivity in biological tissues at both super- and sub-zero temperatures". *Cryobiology*.

[17] Xu, X., and Cui, Z. F., 2003. "Modeling of the co-transport of cryoprotective agents in a porous medium as a model tissue". *Biotechnol Prog,* **19**(3), Jan, pp. 972–81.

[18] Abazari, A., Elliott, J., Law, G., and McGann, L., 2009. "A biomechanical triphasic approach to the transport of nondilute solutions in articular cartilage". *Biophysical Journal,* **97**(12), pp. 3054–3064.

[19] Krogh, A., 1919. "The number and distribution of capillaries in muscles with calculations of the oxygen pressure head necessary for supplying the tissue". *Journal of Physiology-London,* **52**(6), May, pp. 409–415.

[20] Bischof, J. C., and Rubinsky, B., 1993. "Microscale heat and mass-transfer of vascular and intracellular freezing in the liver". *Journal Of Heat Transfer-Transactions Of The ASME,* **115**(4), Nov, pp. 1029–1035.

[21] Rubinsky, B., and Pegg, D. E., 1988. "A mathematical-model for the freezing process in biological tissue". *Proceedings of the Royal Society of London Series B-Biological Sciences,* **234**(1276), Aug, pp. 343–358.

[22] Gosden, R. G., Mullan, J., Picton, H. M., Yin, H., and Tan, S.-L., 2002. "Current perspective on primordial follicle cryopreservation and culture for reproductive medicine". *Hum Reprod Update,* **8**(2), pp. 105–10.

[23] Picton, H. M., and Gosden, R. G., 2000. "In vitro growth of human primordial follicles from frozen-banked ovarian tissue". *Mol Cell Endocrinol,* **166**(1), Aug, pp. 27–35.

[24] Tsai, S., Rawson, D., and Zhang, T., 2009. "Development of cryopreservation protocols for early stage zebrafish (danio rerio) ovarian follicles using controlled slow cooling". *Theriogenology,* **71**(8), pp. 1226–1233.

[25] Kedem, O., and Katchalsky, A., 1958. "Thermodynamic analysis of the permeability of biological membranes to non-electrolytes". *Biochim Biophys Acta,* **27**(2), Feb, pp. 229–46.

[26] Benson, C., Liu, C., Gao, D., Critser, E., and Critser, J., 1993. "Determination of the osmotic characteristics of hamster pancreatic islets and isolated pancreatic islet cells". *Cell Transplant,* **2**(6), Nov, pp. 461–5.

[27] Liu, J., Zieger, M., Lakey, J., Woods, E., and Critser, J., 1997. "The determination of membrane permeability coefficients of canine pancreatic islet cells and their application to islet cryopreservation". *Cryobiology,* **35**(1), Aug, pp. 1–13.

[28] Benson, J. D., 2009. "Mathematical problems from cryobiology". PhD thesis, University of Missouri, June.

[29] Levin, R. L., Cravalho, E. G., and Huggins, C. E., 1977. "Diffusion transport in a liquid solution with a moving, semipermeable boundary". *Journal of Heat Transfer-Transactions Of The ASME,* **99**(2), pp. 322–329.

[30] McGrath, J. J., 1985. "Preservation of biological material by freezing and thawing". In *Heat Transfer in Medicine and Biology*, J. J. McGrath and R. C. Eberhart, eds., Vol. 2. Plenum Press, New York, ch. 20.

[31] Toner, M., Tompkins, R. G., Cravalho, E. G., and Yarmush, M. L., 1992. "Transport phenomena during freezing of isolated hepatocytes". *AICHE Journal,* **38**(10), Oct, pp. 1512–1522.

[32] McGrath, J., 1992. "Coupled transport of water and cryoprotective agents across the murine oocyte plasma membrane". *Ninth National Heat Transfer Conference*.

[33] Crank, J., 1957. *The mathematics of diffusion*. Clarendon Press, Oxford.

[34] Maroudas, A., 1970. "Distribution and diffusion of solutes in articular cartilage". *Biophysical Journal,* **10**(5), pp. 365–379.

[35] Page, E., and Bernstein, R. S., 1964. "Cat heart muscle in vitro:V. diffusion through sheet of right ventricle". *Journal Of General Physiology,* **47**(6), pp. 1129–1140.

[36] Rothe, K. F., 1979. "Fractional extracellular-space and fractional water-content of various rat-tissues at different extracellular ph values and in uremia". *Laboratory Animals,* **13**(2), pp. 171–174.

[37] White, H. L., and Rolf, D., 1957. "Whole body and tissue inulin and sucrose spaces in the rat". *American Journal of Physiology,* **188**(1), pp. 151–155.

[38] Toselli, A., and Widlund, O., 2005. *Domain decomposition methods—algorithsm and theory*, Vol. 34 of *Springer Series in Computational Mathematics*. Springer, Berlin.

[39] Gotoh, M., Maki, T., Satomi, S., Porter, J., Bonnerweir, S., Ohara, C. J., and Monaco, A. P., 1987. "Reproducible high-yield of rat islets by stationary invitro digestion following pancreatic ductal or portal venous collagenase injection". *Transplantation,* **43**(5), May, pp. 725–730.

[40] Gao, D., Benson, C., Liu, C., McGrath, J., Critser, E., and Critser, J., 1996. "Development of a novel microperfusion chamber for determination of cell membrane transport properties". *Biophys J,* **71**(1), Jul, pp. 443–50.

[41] Benson, C., and Critser, J., 1994. "Variation of water permeability (L_p) and its activation energy (E_a) among unfertilized golden hamster and ICR murine oocytes". *Cryobiology,* **31**(3), Jun, pp. 215–23.

[42] Barr, L., and Malvin, R. L., 1965. "Estimation of extracellular spaces of smooth muscle using different-sized molecules". *American Journal of Physiology,* **208**(5), pp. 1042–1045.

[43] Bunch, W., and Edwards, C., 1969. "Permeation of non-electrolytes through single barnacle muscle cell". *Journal of Physiology-London,* **202**(3), pp. 683–697.

[44] Armitage, W. J., and Pegg, D. E., 1979. "Contribution of the cryoprotectant to total injury in rabbit hearts frozen with ethylene-glycol". *Cryobiology,* **16**(2), pp. 152–160.

[45] Meryman, H. T., 1971. "Cryoprotective agents". *Cryobiology,* **8**(2), Apr, pp. 173–183.

[46] Pegg, D. E., and Wusteman, M. C., 1977. "Perfusion of rabbit kidneys with glycerol solutions at 5 degrees C". *Cryobiology,* **14**(2), pp. 168–178.

[47] Gao, D. Y., Ashworth, E., Watson, P. F., Kleinhans, F. W., Mazur, P., and Critser, J. K., 1993. "Hyperosmotic tolerance of human spermatozoa: separate effects of glycerol, sodium chloride, and sucrose on spermolysis". *Biol Reprod,* **49**(1), Jul, pp. 112–23.

[48] Toner, M., Cravalho, E. G., Stachecki, J., Fitzgerald, T., Tompkins, R. G., Yarmush, M. L., and Armant, D. R., 1993. "Nonequilibrium freezing of one-cell mouse embryos - membrane integrity and development potential". *Biophysical Journal,* **64**(6), Jun, pp. 1908–1921.

[49] Karlsson, J. O. M., Cravalho, E. G., Rinkes, I. H. M. B., Tompkins, R. G., Yarmush, M. L., and Toner, M., 1993. "Nucleation and growth of ice crystals inside cultured-hepatocytes during freezing in the presence of dimethyl-sulfoxide". *Biophysical Journal,* **65**(6), Dec, pp. 2524–2536.

[50] Karlsson, J., 2004. "Theoretical analysis of unidirectional intercellular ice propagation in stratified cell clusters". *Cryobiology,* **48**(3), pp. 357–361.

[51] Zhang, A., Xu, L. X., Sandison, G. A., and Zhang, J., 2003. "A microscale model for prediction of breast cancer cell damage during cryosurgery". *Cryobiology,* **47**(2), Oct, pp. 143–54.